Wavelet Transform Based Automatic Lesion Detection in Cervix Images Using Active Contour

[1]Rama Praba, P.S. and [2]H. Ranganathan

[1]Department of Electronics and Communication Engineering,
Sathyabama University, Chennai
[2]Rajiv Gandhi College of Engineering, Chennai

ABSTRACT

Colposcopy is a medical diagnostic procedure to examine an illuminated, magnified view of the cervix by a colposcope. Most cases of cervical cancer can be prevented through screening programs aimed at detecting precancerous lesions. Colposcopy cervical images are acquired in raw form which contains major cervix lesions, regions outside the cervix and parts of the imaging devices such as speculum. In this study, a fully automated lesion detection method based on active contour is proposed. To detect the lesion, the active contour method requires an initial mask in the acetowhite region. In the proposed method, the initial contour is automatically obtained based on Discrete Wavelet Transform (DWT). Before feature extraction, a preprocessing method is applied to remove the irrelevant information and specular reflection from the colposcopy cervical images based on Mathematical morphology, Gaussian Mixture Modeling. Then the wavelet features are extracted and the features are used as an input to the K Nearest Neighbour (KNN) to obtain the initial mask. Segmentation results are evaluated on 240 images of colposcopy.

Keywords: Colposcopy, Gaussian Mixture Model, K Means Clustering, Morphological Operations, Discrete Wavelet Transform, K Nearest Neighbor, Active Contour

1. INTRODUCTION

Cervical cancer is the most common form of cancer in women under 35 years of age, worldwide. Kapoor (2008) shown that a World Health Organization study reveals that every year 1, 32,082 women are diagnosed with cervical cancer and 74,118 die from the disease The growing risk of cervical cancer in women in India is 2.4% compared to 1.3% for the world. More than 90% of cervical cancer in India is squamous cell carcinoma type which develops in the ectocervix. Cervical cancer usually develops in women aged 35-55 years. In India, the peak age for cervical cancer incidence is 45-54 years.

To diagnosis the cervical cancer, two methods are available today. They are Pap test and colposcopy. Pap test can only screen for potential problems, not diagnose them. A Pap test is reported as normal (negative) when all the cells are of a healthy size and shape. An abnormal (positive) test is reported if any cells of different sizes or shapes are found. An abnormal Pap test does not mean the patient has cancer. Hence, to determine the cause of abnormalities, the visual inspection of cervix is needed (McKinley Health Center). A colposcope is very similar to a microscope and allows doctors to examine the external genital area (vulva), vagina and cervix with magnification, so that abnormal cells may be more easily identified.

Colposcopic images are characterized by color, texture and relief information. Thus, their automatic analysis is difficult. However, the diagnosis of experts about some much debated images is often different, because of the very high specialization required. Claude *et al.* (2001) reported that an integrated analysis tool for helping gynecologists to build their colposcopic diagnosis is proposed. Moreover, specific preprocessing methods and different segmentation methods are available like principal component analysis and multidimensional histogram analysis.

Gordon and Greenspan (2007) reported that in cervigram, the lesions are of varying sizes and complex,

---

Corresponding Author: Rama Praba P.S., Department of Electronics and Communication Engineering, Sathyabama University, Chennai

non-convex shapes. A new methodology that enables the segmentation of non-convex regions, thus providing a major step forward towards cervigram tissue detection and lesion description is presented. The framework transitions from pixels to a set of small coherent regions, which are grouped bottom-up into larger, non-convex, perceptually similar regions, utilizing a new graph-cut criterion and agglomerative clustering. Greenspan *et al.* (2009) reported that a multistage scheme for segmenting and labeling regions of anatomical interest within the cervigrams is presented. In particular, focus on the extraction of the cervix region and fine detection of the cervix boundary; specular reflection is eliminated as an important preprocessing step and in addition, the entrance to the endocervical canal is detected.

Claude *et al.* (2002) reported that colposcopic image classification based on contour parameters using different artificial neural network and the KNN classifier is proposed. A set of original spatial and frequency parameters is extracted from 283 samples to characterize the attribute of contour. Tulpule *et al.* (2005) reported that the spatial parameter is the number of the region around the edges and the frequency parameters are amplitude of first peak, frequency of the end of first peak, area under first peak and area under other peaks. Then the Principal Component Analysis is performed to test the parameters. Segmentation and classification of cervix lesions by pattern and texture analysis is presented. The acetowhite region, a major indicator of abnormality in the cervix image, is first segmented by using a non-convex optimization approach. Within the acetowhite region, other abnormal features such as the mosaic patterns are then automatically classified from non-mosaic regions by texture analysis.

Artan and Huang (2008) reported that a cost-sensitive 2ν-SVM classification scheme to cervical cancer images to separate diseased regions from healthy tissue is proposed. Multiplier classifier scheme is used instead of the traditional single classifier to test the NCI/NLM archive of 60000 images. Acosta-Mesa *et al.* (2005) stated that the phase correlation method followed by a locally applied algorithm based on the normalized cross-correlation is presented for image registration. During the parameterization process, each time series obtained from the image sequences is represented as a parabola in a parameter space. A supervised Bayesian learning approach is proposed to classify the features in the parameter space according to the classification made by the colposcopist.

Srinivasan *et al.* (2009) reported that Cervical Intraepithelial Neoplasia (CIN) is detectable and treatable precursor pathology of cancer of the uterine cervix. A non-parametric technique, based on the transformation and analysis of the distortion-rate curve is proposed. To assess the model order this technique provides good starting points to infer the GMM parameters via the Expectation-Maximization (EM) algorithm, reducing the segmentation time and the chances of getting trapped in local optima.

Meslouhi *et al.* (2009) reported that the proposed automatic lesion detection method in cervical images uses region based active contour segmentation. The region based active contour segmentation method requires an initial curve or mask to segment the given image. To detect the lesion, the initial mask must be in the acetowhite region. In the propose method, the initial mask is automatically generated based on discrete wavelet transform whereas, the initial mask is manually selected.

2. MATERIALS AND METHODS

2.1. Initial Mask Generation

Colposcopy cervical images are acquired in raw form which contains major cervix lesions, regions outside the cervix and parts of the imaging devices such as speculum. Before generating the initial mask, the region of interest is identified and specular reflection is removed.

2.2. ROI Segmentation of Cervical Images

The segmentation of cervix from the colposcopy cervix image is shown in **Fig. 1**. An ROI segmentation image processing system substantially masks non-ROI image data from a digital image to produce a ROI segmented image for subsequent digital processing. A colposcopy cervical image contains major cervix lesions, regions outside the cervix and parts of the imaging device. In this method, only the major cervix lesion is segmented for further processing. The major cervix lesion is a reddish, nearly circular section approximately centered in the image. This feature is used to identify the ROI region.

For ROI segmentation, first the given cervix image in RGB colour space is converted into Lab colour space due to the fact that Lab colour space is a good choice for representing the colour. The Euclidean distance of a pixel from the image center is extracted for all pixels and it is represented as Euclidean distance array d. The Gaussian Mixture Model (GMM) parameters μ and σ are calculated in Equation 1 for the Euclidean distance array and the colour channel a from the Lab colour space:

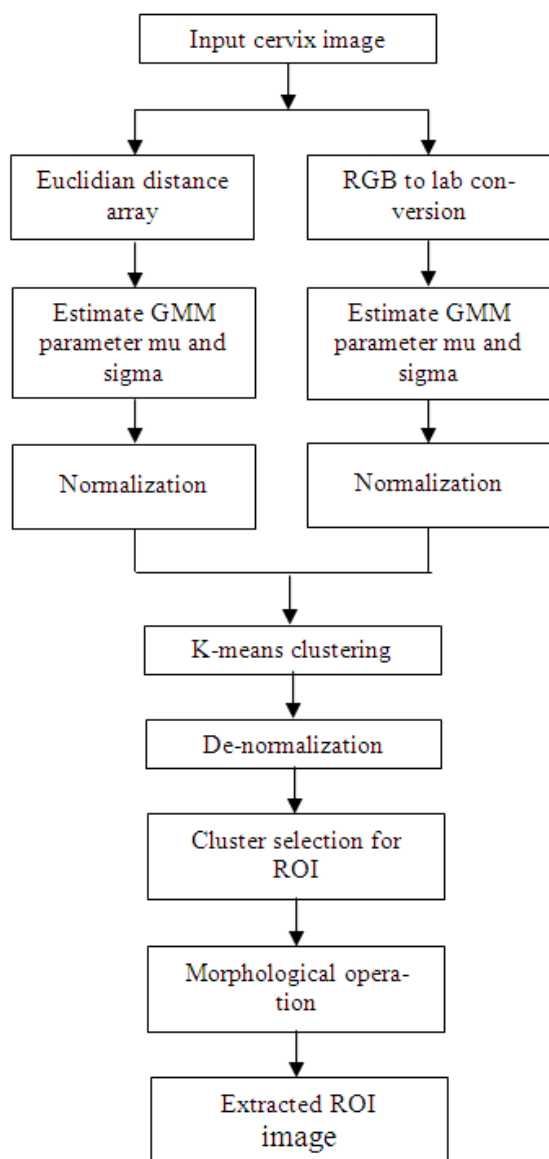$$a(x,y) = \frac{a - \mu_a}{\sigma_a} \text{ and } d(x,y) = \frac{d - \mu_d}{\sigma_d} \tag{1}$$

Fig. 1. Block diagram of ROI Segmentation of cervical images

By using the GMM parameters, Euclidean distance array and the colour channel a from the Lab colour space are normalized and aggregated into a single array which is given to K-means clustering algorithm as an input. Here the value K is set to 2. Among the 2 cluster, the cluster which has the smallest d and largest is chosen as ROI after the cluster centroids are de-normalized. Finally, morphological opening is used to remove the small regions and fill the holes to get the required ROI image that contains only the cervix lesion.
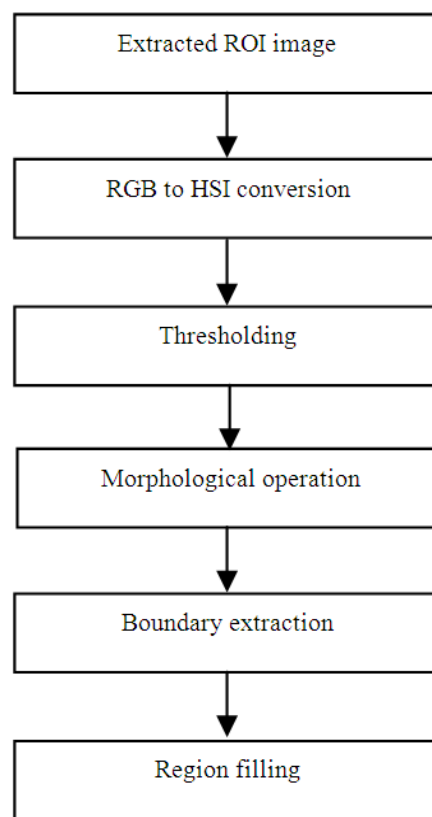

Fig. 2. Block diagram for removing Specular Reflection on ROI cervix images

2.3. Specular Reflection of Cervical Images

Specular Reflections (SR) appear as bright spots heavily saturated with white light. These occur due to the presence of moisture on the uneven cervix surface, which acts like mirrors reflecting the light from the illumination source. The block diagram for removal of specular reflection in the segmented cervix image is shown in **Fig. 2**. The segmented cervix image in RGB colour space is converted into HSI colour space due to the fact that HSI colour space represents the colour similarity how the human eye senses colours. The HSI color model represents every color with three components, Hue (H), Saturation (S) and Intensity (I). Specularities always have very intense brightness and low saturation values. Hence, I and S component in the HSI colour space is used to find the SR region and the conversion formulae are given in Equation 2 and 3 respectively:
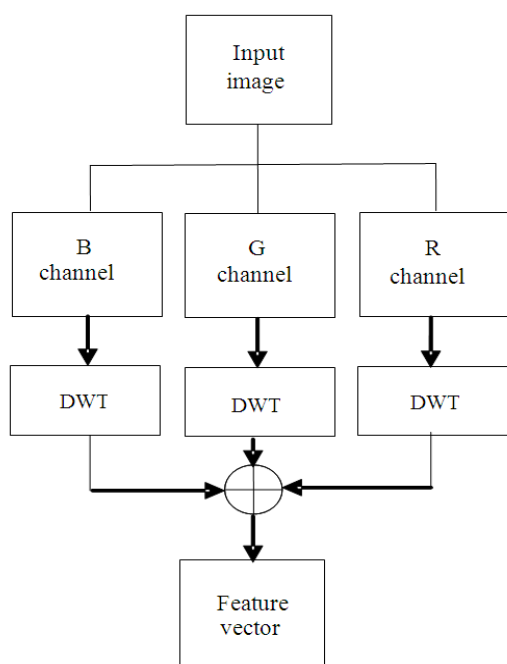
$$I = \frac{R + G + B}{3} \tag{2}$$

Fig. 3. Block diagram of feature extraction stage

$$S = 1 - \frac{\min(R, G, B)}{3} \tag{3}$$

The initial SR regions are identified by applying thresholding technique on image pixels. The threshold values are defined in Equation 4:

$$I \rangle 0.8 * I_{max} \quad S \rangle 0.6 * S_{max} \tag{4}$$

After thresholding, morphological dilation is performed on the thresholded image by using square structuring element of width 5 to get SR regions. Boundaries are extracted from the SR regions by using 8-connected neighborhood. Finally, the SR regions are smoothly interpolates inward from the pixel values on the boundaries by solving Laplace's equation.

2.4. Mask Identification

The mask identification mainly consists of two stages namely feature extraction stage and classification stage. In the feature extraction stage, the wavelet coefficients are extracted from the normal and abnormal region and these features are given to the KNN classifier for generating the initial mask.
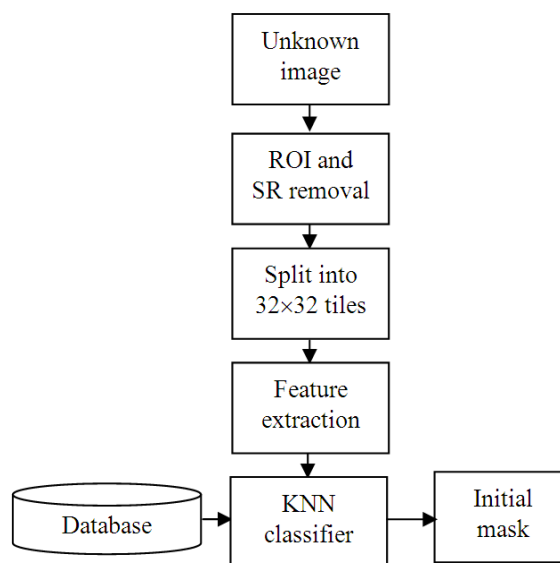

Fig. 4. Block diagram of initial mask identification stage

2.5. Feature Extraction Stage

For feature extraction, 20 normal and 20 abnormal cervix images marked by the experts are taken. The normal and abnormal region in cervix images is divided into 32×32 non overlapping tiles. R, G and B channel of every tile is decomposed by using discrete wavelet transform. The wavelet coefficients are used as features. Then, the features of R, G and B channel is fused together to form the Feature vector (F) and stored in the database which will be used for training the classifier. The feature extraction stage is shown in **Fig. 3**.

2.6. Identification Stage

The initial mask identification stage is shown in **Fig. 4**. The given unknown image is divided into 32×32 non overlapping tiles. For each tiles, the wavelet features are calculated and processed with the Feature vector (F). Then, each tile is classified using a KNN classifier as normal or abnormal. The distance measure used in KNN classifier is Euclidean distance.

2.7. Lesion Detection

In the proposed method, active contour method is used to detect the lesion. The mask obtained from the initial mask identification system is given to the active contour segmentation method as initial contour. The mathematical background of active contour is summarized as follows.

Let us define the evolving curve C in Ω, as the boundary of an open subset ω of Ω and inside (C) denotes the region ω and outside (C) denotes the region $\frac{\Omega}{\omega}$. The Active contour method in (Chan and Vese, 2001) is the minimization of energy based segmentation. Assume that the image u_0 is formed by two regions of approximatively piecewise-constant intensities, of distinct values u_0^i and u_0^o. Assume further that the object to be detected is represented by the region with the value u_0^i. Let denote its boundary by C_0. Let us consider the following "fitting" term in Equation 5:

$$F_1(C) + F_2(C) = \int_{inside(c)} \left| u_0(x,y) - c_1 \right|^2 dxdy$$
$$+ \int_{outside(c)} \left| u_0(x,y) - c_2 \right|^2 dxdy \qquad (5)$$

where, C is any other variable curve and the constants c_1, c_2 depending on C, are the averages of u_0 inside C and respectively outside C. In this simple case, it is obvious that C_0, the boundary of the object is the minimizer of the fitting term Equation 6:

$$\underset{c}{\inf} \{ F_1(C) + F_2(C) \} \approx 0 \approx F_1(C_0) + F_2(C_0) \qquad (6)$$

For instance, if the curve C is outside object, then F_1 (C)>0 and F_2 (C) $\approx$ 0. If the curve C is inside the object, then F_1 (C) $\approx$ 0 and F_2 (C)>0. If the curve C is both inside and outside the object, then F_1 (C)>0 and F_2 (C) $\approx$ 0. Finally, the fitting energy is minimized if C = C_0, i.e., if the curve C is on the boundary of the object.

In the active contour model, the minimization of the above fitting term and also add some regularizing terms, like the length of the curve C and (or) the area of the region inside. Therefore, the energy functional (c_1, c_2, C), defined in Equation 7:

$$F(c_1, c_2, C) = \mu.Length(C) + v.Area(inside(C))$$
$$+ \lambda_1 \int_{inside(c)} \left| u_0(x,y) - c_1 \right|^2 dxdy \qquad (7)$$
$$+ \lambda_2 \int_{outside(c)} \left| u_0(x,y) - c_2 \right|^2 dxdy$$

where, $\mu \geq 0$, $v \geq 0$, λ_1, $\lambda_2 > 0$ are fixed parameters. In [XX], λ_1, $\lambda_2 = 1$ and v = 0 Therefore, the minimization problem is given in Equation 8:

$$\underset{c_1, c_2, C}{\inf} F(c_1, c_2, C) \qquad (8)$$

The Mumford-Shah functional for segmentation is given in Equation 9:

$$F^{MS}(u, C)$$
$$= \mu.Length(C) + \lambda \int_{\Omega} \left| u_0(x,y) - u(x,y) \right|^2 \qquad (9)$$
$$+ \int_{\Omega_c} \left| \nabla u(x,y) \right|^2 dxdy$$

where, $u_0 : \bar{\Omega} \to R$ is a given image, μ and λ are positive parameters. The solution image u obtained by minimizing this functional is formed by smooth regions R_i and with sharp boundaries, denoted by C.

A reduced form of this problem is simply the restriction of F^{MS} to piecewise constant functions u, i.e., u = cons tan tc_i on each connected component R_i of $\frac{\Omega}{C}$. Therefore, as it was also pointed out in (Mumford and Shah, 1989), c_i = average (u_0) on each connected component R_i. The reduced case is called the minimal partition problem. The active contour model with v = 0 and $\lambda_1 = \lambda_2 = \lambda$ is a particular case of the minimal partition problem, in which for the best approximation u of u_0 as a function taking only two values, namely Equation 10:

$$u = \begin{cases} average \ (u_0) \ inside \ C \\ average \ (u_0) \ outside \ C \end{cases} \qquad (10)$$

And with one edge C, represented by the snake or the active contour.

This particular case of the minimal partition problem can be formulated and solved using the level set method. In the level set method (Osher and Sethian, 1988), C is represented by the zero level set of a Lipschitz function $\varphi : \Omega \to R$, such that Equation 11:

$$\begin{cases} C = \partial\omega = \{ (x,y) \in \Omega : \varphi(x,y) = 0 \} \\ inside(C) = \omega = \{ (x,y) \in \Omega : \varphi(x,y) > 0 \} \\ outside(C) = \Omega \setminus \bar{\omega} = \{ (x,y) \in \Omega : \varphi(x,y) < 0 \} \end{cases} \qquad (11)$$

Consequently the function ϕ becomes the required unknown factor minimizing the energy. By introducing the Heaviside function H and the Dirac δ_0 defined respectively in Equation 12-14:

$$H(z) = \begin{cases} 1, \ if \ z \geq 0 \\ 0, \ if \ z < 0 \end{cases} \quad \delta_0(z) = \frac{d}{dz} H(z) \qquad (12)$$

The energy function becomes (Srinivasan *et al*., 2009):

$$F(c_1,c_2,\varphi) = \mu \int_\Omega \delta\big(\varphi(x,y)|\nabla\varphi(x,y)|dxdy$$
$$+ v \int_\Omega H(\varphi(x,y)dxdy$$
$$+ \lambda_1 \int_\Omega |u_0(x,y)-c_1|^2 H(\varphi(x,y)dxdy$$
$$+ \lambda_2 \int_\Omega |u_0(x,y)-c_2|^2 (1-H(\varphi(x,y))dxdy$$

(13)

To compute Euler-Lagrange equations for the unknown function φ, consider the regularized versions of functions H and δ_0 denoted by H_ϵ and δ_ϵ as $\in \rightarrow 0$ and finally the equation of evolution is directly expressed with the function of level sets φ (Srinivasan *et al*., 2009):

$$\frac{\partial \varphi}{\partial t} = \delta_\epsilon(\varphi)\left[\begin{array}{c}\mu \operatorname{div}\left(\dfrac{\nabla\varphi}{|\nabla\varphi|}\right)-v-\lambda_1 \\ (u_0-c_1)^2+\lambda_2(u_0-c_2)^2\end{array}\right]$$
$$= 0 \text{ in } (0,\infty)\times\Omega,\varphi(0,x,y)$$
$$= \varphi_0(x,y)\text{ in }\Omega,\frac{\delta_\epsilon(\varphi)}{|\nabla\varphi|}\frac{\partial\varphi}{\partial\vec{n}}$$
$$= 0 \text{ on } \partial\Omega$$

(14)

where, $\vec{n}$ denotes the exterior normal to the boundary $\partial\Omega$ and $\dfrac{\partial\varphi}{\partial\vec{n}}$ denotes the normal derivative of φ at the boundary.

3. RESULTS AND DISCUSSION

3.1. Experimental Results

The performance of the proposed method is tested on 200 normal colposcopy cervix images and 40 abnormal colposcopy cervix image obtained from Government Kasturibaigandhi Hospital (KGH), Chennai, India. Experimental result of 3 cervix images by the proposed system is shown in **Fig. 5**. The First row image in the figure is normal cervix image. There is no initial mask is obtained from the mask identification system. Hence, the given image is considered as normal and there is no mark by the proposed method and the expert also. The second row image does not contain any parts of the imaging devices and speculum reflections. The detected lesions in the second and third row images are similar to the experts' results. **Table 1** shows the performance of the proposed system for 5 images in terms of specificity, sensitivity, classification accuracy, Positive Predictive Value (PPV) and Negative Predictive Value (NPV).
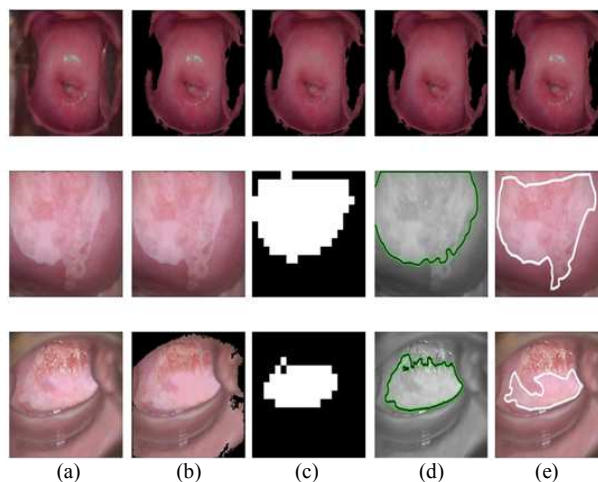

(a)   (b)   (c)   (d)   (e)

Fig. 5. (a) Input Image (b) ROI segmentation and SR removal (c) initial mask (d) Proposed method (e) Marked by expert

Table 1. Performance measure of the proposed lesion detection method

Image	Sensitivity	Specificity	Accuracy	PPV	NPV
1	0.79	0.95	92.90	0.75	0.96
2	0.64	0.82	72.57	0.78	0.69
3	0.98	0.92	92.80	0.66	0.99
4	0.93	0.84	88.88	0.87	0.91
5	0.53	1.00	80.93	1.00	0.76
Avg	0.77	0.91	85.62	0.81	0.86

4. CONCLUSION

In this study, a fully automated method for lesion detection in cervix images based on active contour method is proposed. The initial mask required by the active contour method is automatically obtained by using wavelet features. The purpose of the recommended process is mainly to prepare the colposcopy cervix images for further analysis. The sensitivity, specificity and classification accuracy of the proposed lesion detection method is 0.77, 0.91 and 85.62 respectively. The proposed algorithm is tested on a large set of images totally 240 images and good results are achieved.

5. REFERENCES

Acosta-Mesa, H.G., Z. Barbara, H.V. Rios-Figueroa, N. Cruz-Ramirez and A. Marin-Hernandez, 2005. Cervical cancer detection using colposcopic images: A temporal approach. Proceedings of the IEEE International Conference on Computer Science, Sept. 26-30, IEEE Xplore Press, pp: 158-164. DOI: 10.1109/ENC.2005.14

Artan, Y. and X. Huang, 2008. Combining multiple 2v-svm classifiers for tissue segmentation. Proceedings of the 5th IEEE International Symposium on Biomedical Imaging, May 14-17, IEEE Xplore Press, Paris, pp: 488-491. DOI: 10.1109/ISBI.2008.4541039

Chan, T.F. and L.A. Vese, 2001. Active contours without edges. IEEE Trans. Image Proces., 10: 266-277. DOI: 10.1109/83.902291

Claude, I., P. Pouletaut, S. Huault and J.C. Boulanger, 2001. Integrated color and texture tools for colposcopic image segmentation. Proceedings of the IEEE International Conference on Image Processing, Oct. 7-10, IEEE Xplore Press, Thessaloniki, pp: 311-314. DOI: 10.1109/ICIP.2001.958490

Claude, I., R. Winzenrieth, P. Pouletaut and J.C. Boulanger, 2002. Contour features for colposcopic image classification by artificial neural networks. Proceedings of the 16th IEEE International Conference on Pattern Recognition, (ICPR' 02), IEEE Xplore Press, pp: 771-774. DOI: 10.1109/ICPR.2002.1044872

Gordon, S. and H. Greenspan, 2007. Segmentation of non-convex regions within uterine cervix images. Proceedings of the IEEE 4th International Symposium on Biomedical Imaging, Apr. 12-15, IEEE Xplore Press, Arlington, VA., pp: 312-315. DOI: 10.1109/ISBI.2007.356851

Greenspan, H., S. Gordon, G. Zimmerman, S. Lotenberg and J. Jeronimo et al., 2009. Automatic detection of anatomical landmarks in uterine cervix images. IEEE Trans. Med. Imag., 28: 454-468. DOI: 10.1109/TMI.2008.2007823

Kapoor, D., 2008. All about India's commonest cancer: Cervical cancer.

Meslouhi, O.E., M. Kardouchi, H. Allali and T. Gadi, 2009. Semi-automatic cervical cancer segmentation using active contours without edges. Proceedings of the 5th International Conference on Signal Image Technology and Internet Based Systems, Nov. 29-Dec. 4, IEEE Xplore Press, Marrakesh, pp: 54-58. DOI: 10.1109/SITIS.2009.19

Mumford, D. and J. Shah, 1989. Optimal approximations by piecewise smooth functions and associated variational problems. Commun. Pure Applied Math., 42: 577-685. DOI: 10.1002/cpa.3160420503

Osher, S. and J.A. Sethian, 1988. Fronts propagating with curvature-dependent speed: Algorithms based on hamilton-jacobi formulations. J. Comput. Phys., 79: 12-49. DOI: 10.1016/0021-9991(88)90002-2

Srinivasan, Y. and E. Corona, B. Nutter, S. Mitra and S. Bhattacharya, 2009. A unified model-based image analysis framework for automated detection of precancerous lesions in digitized uterine cervix images. IEEE J. Selected Topics Signal Process., 3: 101-111. DOI: 10.1109/JSTSP.2008.2011102

Tulpule, B., S. Yang, Y. Srinivasan, S. Mitra and B. Nutter, 2005. Segmentation and classification of cervix lesions by pattern and texture analysis. Proceedings of the IEEE 14th International Conference on Fuzzy System, May 25-25, IEEE Xplore Press, Reno, NV., pp: 173-176. DOI: 10.1109/FUZZY.2005.1452388